Multi-Channel HTS rf SQUID Gradiometer System Recording Fetal and Adult Magnetocardiograms

Yi Zhang, Norbert Wolters, Dieter Lomparski, Willi Zander, Marko Banzet, Jürgen Schubert, Hans-Joachim Krause, and Peter van Leeuwen

***Abstract*—We report on experiments with a multi-channel HTS radio-frequency (rf) SQUID gradiometer for recording fetal and adult magnetocardiograms. Four sensing SQUID magnetometers and two common reference SQUID magnetometers form a 4 channel electronic gradiometer system of either first or second order. The magnetometers consist of HTS step edge SQUIDs and flux concentrators fabricated from YBaCuO thin films, with dielectric substrate resonators serving as tank circuits. With a washer area of 18 mm in diameter, all six magnetometers reached a field sensitivity of 20–30 $\mathrm{fT}/\sqrt{\mathrm{Hz}}$. Each gradiometer channel is formed using two or three such magnetometers with individual readouts in electronic difference. The dc and rf crosstalk between any channel pair was measured. In ordinary operation we did not find any noise contribution from neighboring channels, even though the resonant frequencies of the resonators are closely spaced. In a standard magnetically shielded room, using a first-order gradiometer configuration with an ultra-long baseline of about 20 cm, we demonstrated 4 channel real-time heart signal recordings of a fetus in the 33rd week of gestation.**

***Index Terms*—Biomagnetics, SQUIDs.**

I. Introduction

MAGNETOCARDIOGRAPHY (MCG) using High Temperature Superconductor (HTS) Superconducting QUantum Interference Device (SQUID) magnetometers and electronic gradiometers not only inside but also outside magnetically shielded rooms (MSR) has been demonstrated over the last 10 years [1]–[4]. Recently, we have discussed the influences of the gradiometer baseline length on a human heart measurement when performing MCG mappings using our single-channel radio-frequency (rf) SQUID gradiometer. It was found that MCG mappings recorded by a gradiometer yield distorted magnetic field maps in comparison to magnetometer mappings. The distortion was weaker for the first-order gradiometers than for the second-order gradiometer. Using a first-order gradiometer with ultra-long baseline of 18 cm in a standard MSR, we were able to record, for the first-time, fetal MCG signals in real time [5].

The interest in using MCG and fetal MCG as a diagnostic tool has increased [6]. Preferably, MCG maps should be simultaneously recorded by multi-channel systems at typically 36 or more positions in a plane close to the subject's torso [7]. Multi-channel MCG systems using Low Temperature Superconductor (LTS) SQUID are entering the medical market. Tsukamoto *et al.* have already reported on multi-channel HTS dc SQUID systems for MCG evaluation [8]. Recently, Suduki *et al.* extended the number of channels up to 51 [9].

In this work, we report on MCG experiments performed using our multi-channel HTS rf SQUID gradiometer. In a standard MSR, using a first-order gradiometer configuration with ultra-long baseline of 20 cm, we performed four-channel heart signal recordings of a 33 week-old fetus and obtained good-quality real time signals.

Manuscript received October 3, 2004.

Y. Zhang, N. Wolters, D. Lomparski, W. Zander, M. Banzet, J. Schubert, and H.-J. Krause are with the Institut für Schichten und Grenzflächen (ISG-2), D 52425 Jülich, Germany (e-mail: y.zhang@fz-juelich.de).

P. van Leeuwen is with the Entwicklungs-und Forschungszentrum für MikroTherapie gGmbH (EFMT), D 44799 Bochum, Germany.

Digital Object Identifier 10.1109/TASC.2005.849974

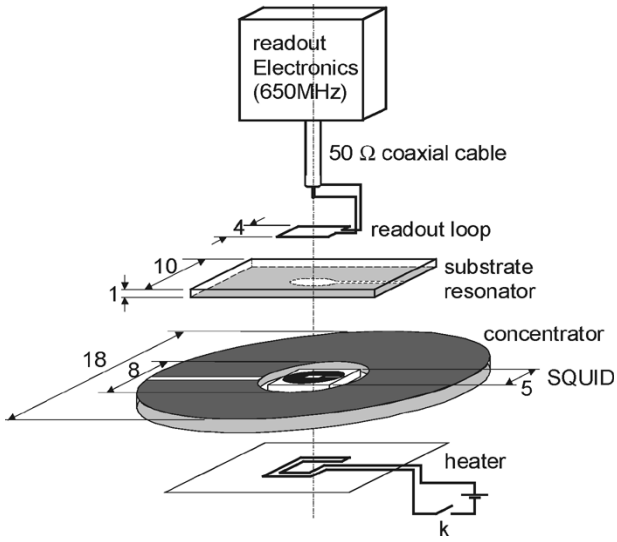

Fig. 1. rf SQUID magnetometer module.

II. rf SQUID Magnetometer Module

The HTS electronic gradiometer consists of SQUID magnetometers. Therefore, the intrinsic noise of magnetometers is an important factor for gradiometer performance. For optimum rf SQUID operation, one also needs a high-performance resonator (tank circuit) that combines a high resonance frequency f_0, a high unloaded quality factor Q_0, with a strong confinement of the spatial distribution of the rf energy.

In order to meet these performance requirements, we have developed a radio-frequency (rf) SQUID magnetometer with a $SrTiO_3$ substrate serving simultaneously as tank circuit (dielectric resonator) and flux focuser [10].

Each magnetometer used for the purpose of this work (see Fig. 1) consists of

1) SQUID chip: The SQUID chip consists of a 5 mm × 5 mm substrate with a 200 nm deep ditch, such that a step-edge grain-boundary junction forms an epitaxial YBCO thin film micro-bridge when deposited and patterned over the ditch. The SQUID layout is patterned in the YBCO film to form our standard 3.5 mm diameter washer with a 100 μm × 100 μm SQUID loop. The field-to-flux coefficient of the bare SQUID is about 10 nT/Φ_0.
2) Dielectric resonator chip: We used a standard $\mathrm{SrTiO_3}$ substrate with dimensions $10 \times 10 \times 1\ \mathrm{mm}^3$. A YBCO thin film SQUID washer-structure flux concentrator is patterned on it. It serves as tank circuit (resonator) and as a flux focuser. The resonance frequency $\mathrm{f_0}$ is about 650 MHz at 77 K. In flip-chip configuration with (1), it improves the field-to-flux coefficient to 3.2 nT/Φ_0.
3) Large flux concentrator ring: On a circular $\mathrm{LaAlO_3}$ substate with a diameter of 18 mm and an inner borehole of 8 mm diameter, epitaxial YBCO is deposited and a flux focuser structure is patterned. The SQUID chip is positioned in the center bore of the concentrator, see Fig. 1. It further reduces the field-to-flux coefficient to 2 nT/Φ_0.
4) Patterned readout loop: It is placed on the opposite side of the resonator chip and is connected to the SQUID readout electronics by only one 50 Ω coaxial cable. The rf pumping current and feedback flux are applied via the readout loop.

The SQUID chip, the resonator chip, the flux concentrator chip, the readout loop, and a planar resistive heater for flux expulsion are encapsulated in a fiberglass enclosure to form a magnetometer module.

All six magnetometers exhibited a field sensitivity of 20–30 $\mathrm{fT}/\sqrt{\mathrm{Hz}}$. Each one of the four gradiometer channels is formed using two (first-order) or three (second-order gradiometer) such magnetometers with individual readouts in electronic difference.

III. Electronic Gradiometer

Because it is not possible to build a gradiometer with a HTS axial gradiometric pick-up loop, a reduction of the total magnetometer number is our basic concern in the development of a multi-channel gradiometer system. Our system is constructed with four sensing SQUID magnetometers and only one common reference magnetometer for the first-order gradiometer or two common reference magnetometers for the second-order gradiometer configuration.

The arrangement of all 6 magnetometers is shown in Fig. 2. Four sensing magnetometer (A1, A2, A3, A4) are located at the bottom of the dewar on the 4 corners of a 4 cm × 4 cm square. The z-axis along which two reference magnetometers are mounted runs through the center of the square and is perpendicular to it. The reference magnetometer B defines the middle plane, the reference magnetometer C is located in the top plane. The spacing L of neighboring planes is 10 cm.

We analyzed four electronic configurations: 1) M(A); a single magnetometer A. 2) $\mathrm{G1(A-B)}$; first order gradiometer with a baseline of 10 cm. 3) $\mathrm{G1(A-C)}$; first order gradiometer with a baseline of 20 cm. 4) $\mathrm{G2(A-2B+C)}$; second order gradiometer with a baseline of 2 × 10 cm. The configuration can be changed in situ during the measurement.

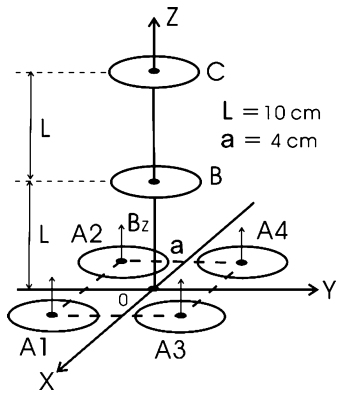

Fig. 2. The arrangement of the four sensing magnetometers (A1, A2, A3, A4) and the two reference magnetometers (B, C).

Because of differences in the mutual inductance M between SQUID and readout loop, the voltage-to-field coefficients $\partial \mathrm{V}/\partial \mathrm{B}$ of magnetometers in the flux-locked loop have a small difference as well. In order to achieve the best balance of a gradiometer, one should adjust the balance factor k for each gradiometer output of e.g. $(\mathrm{A} - k\mathrm{C})$. In our design, the voltage-to-field coefficient $\partial \mathrm{V}/\partial \mathrm{B}$ of any sensing magnetometer is considered the standard value for this gradiometer, while the $\partial \mathrm{V}/\partial \mathrm{B}$ of the reference magnetometer is variable with a balance factor k between 0.7 and 1.4.

IV. Crosstalk Measurements

The measurement of crosstalk between each channel is also a very important characterization for a multi-channel system. It characterizes the independence of the individual channels. For an rf SQUID system, one expects to observe not only low-frequency (dc) crosstalk, but also radio frequency (rf) crosstalk.

A. dc Crosstalk

At first, we measured the current to generate a single flux quantum, $\mathrm{I}(\Phi_0)$, and its corresponding output voltage, $\mathrm{V}(\Phi_0) = \mathrm{I}(\Phi_0) \times \mathrm{R_f}$ (feedback resistor), of a magnetometer in a flux-locked loop. In order to measure the dc crosstalk between the Channels, a large current corresponding to a flux change of 1000 flux quanta was applied to the readout loop of one magnetometer and the response measured with a locked neighboring channel was recorded. In these measurements, we used a current with a low frequency of 5 Hz. The dc crosstalk between arbitrary channel pairs was found to be in the 10^{-5} range. In MCG measurements, the flux change is less that one Φ_0. Therefore, the influence of dc crosstalk is insignificant during normal operation.

B. rf Crosstalk

In order to measure the rf crosstalk, we determined the resonant frequency $\mathrm{f_0}$ and the operating rf power $\mathrm{P_0}$ of one channel. Then, this channel was operated in a flux-locked loop. An rf current having the same frequency $\mathrm{f_0}$ was sent to a neighboring channel via the corresponding cables and readout loops. The

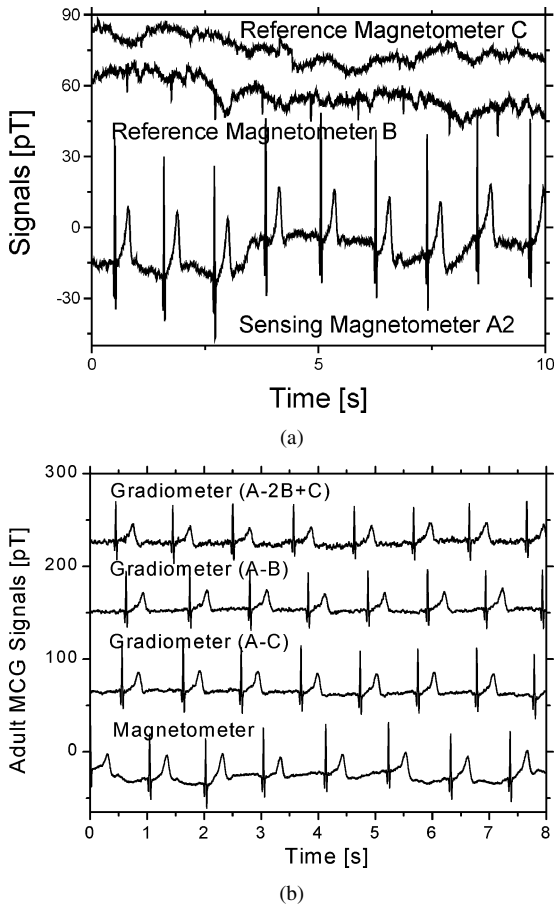

Fig. 3. (a) Human heart signals recorded with 3 magnetometers in different planes. The frequency range of all the measurements in Fig. 3 (a) and (b) was 0.02 Hz to 80 Hz, with a 50 Hz notch filter. (b) Adult heart signals recorded using 3 different gradiometers and a magnetometer.

power of the rf generator was then increased until the real time peak-to-peak noise of the operating channel increased by about 10%. We define the ratio of the operating rf power P_0 to this particular rf power level as rf crosstalk. We found, that the rf crosstalk does not depend on the distance between channels. The rf crosstalk level ranged from -60 dBm to -70 dBm. This power level is still 2 to 3 orders of magnitude higher than the operating rf power of -90 dBm. Furthermore, all the six magnetometers always have different resonant frequencies f_0, although they have the same configuration. The variation of f_0 for the six channels is about 15%. Because of the small operating rf power (-90 dBm) and different resonant frequencies f_0, an rf crosstalk problem has never occurred in our system during normal operation.

V. Influence of Baseline on Adult MCG

We performed MCG measurements on adult subjects in our MSR using the described system. In order to study the influence of the baseline dependence on the MCG signals, we measured at one sensor position (A2 in Fig. 2), where we found the maximal signal, using different configurations. Fig. 3(a) shows the human heart signals measured with 3 magnetometers, A, B, C, positioned at their planes along the z-axis. For the individual magnetometers A, B, C, the amplitudes of the QRS complex are 75 pT, 13 pT and smaller than 5 pT, respectively. The distance

Fig. 4. A pregnant woman in supine position under the system dewar and gantry. The fetal heart signals were found on the right hand side of the mother's abdomen.

between A2 and the torso surface was approximately 3 cm. In theory, we can calculate the effective area of a dipole, which serves as the physical model of a human heart.

From the traces shown in Fig. 3(b), one infers that, in our MSR, the gradiometer noise does not depend on the baseline distance, and the first order gradiometer $G1(A - C)$ with a base line of 20 cm achieved the best signal-to-noise ratio (SNR). $G2\ (A - 2B + C)$ has the worst SNR.

For MCG measurements one needs a reference (standard) signal. This should be the signal measured with a magnetometer, because the amplitude reduction recorded using gradiometers depends on the arbitrary gradiometer configuration and mapping position. In our previous work, we have discussed this in detail [5].

If the reference magnetometer is located at a distance where the signal of the human heart is smaller than our system noise. the system behaves like an ideal gradiometer. Here the baseline length may be more than 35 cm.

The long baseline has the additional advantage of reducing the influence of other gradient fields, $\partial B_Z/\partial x$ and $\partial B_Z/\partial_y$, because the sensing magnetometers and the reference magnetometers are not located along the same axis in z direction in our arrangement (see Fig. 2). Indeed, the influence of $\partial B_Z/\partial x$ and $\partial B_Z/\partial y$ is reduced by a factor of $(x^2 + y^2)^{1/2}/L$, where L is the baseline length. Of course, this influence disappears when we use an ideal gradiometer.

VI. Fetal MCG Measurement

Prenatal acquisition of the electrocardiogram (ECG) being notoriously difficult, fetal MCG is an important alternative for the registration of fetal cardiac activity [11]. As it has been shown that consistent data analysis is difficult using single channel systems, there is a need for multi-channel equipment [12].

The volume of a fetal heart is much smaller than that of an adult. The magnetic signal reduces dramatically with increasing distance between the heart and the sensor. For a fetal MCG recording, our gradiometer with 20 cm baseline comes closer to an ideal gradiometer. We have conducted fetal MCG measurements in our MSR in Jülich. The fetal MCG recordings were done with only the first-order gradiometer with 20 cm baseline, $G1(A - C)$, of a fetus in the 33rd week of gestation. The fetal

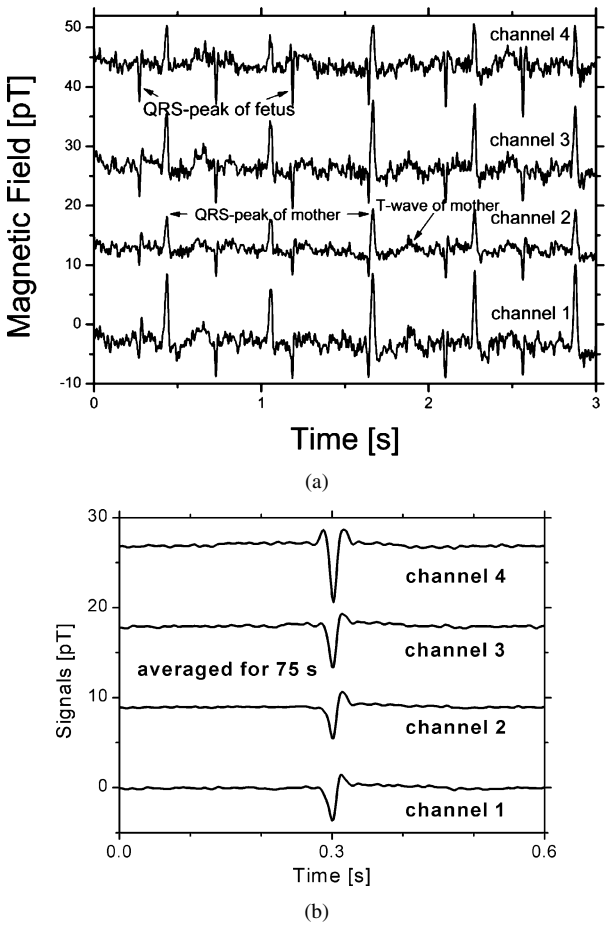

Fig. 5. (a) All the four first-order gradiometers with 20 cm baseline recorded clear fetal MCG signals in real time. (b) Fetal MCG signals averaged over 75 s.

heart signals were found on the right hand side of the mother's abdomen (see Fig. 4). Because our system cannot be tilted, the signal-to-noise ratio could be probably optimized further.

The measured real-time traces (Fig. 5(a)) of four channels exhibit both the fetal heart signal and the maternal heart signal. The SQUID gradiometer system noise was about 1.5 pT peak-to-peak with a video bandwidth of 90 Hz. For channel 4, the QRS peak of the fetal heart beat was about 7.5 pT, resulting in a SNR of about 5 in the real-time data. The standard procedure to enhance the SNR was used here: the maternal heart beats were identified by correlation analysis, averaged and subtracted. In the resulting signal, all the fetal beats were identified and beats which correlated well with the fetal QRS template were averaged over 75 s, see Fig. 5(b).

VII. Conclusion and Outlook

In conclusion, we have constructed a multi-channel gradiometer system consisting of four HTS rf SQUID sensing magnetometers and two common reference magnetometers. The system can be operated in different gradiometer configurations. Using four-channel first-order gradiometers with an ultra-long baseline of 20 cm in a standard MSR, we obtained the adult heart signal with the best SNR, as compared to other gradiometer configurations. We measured fetal MCG signals in the 33rd week of gestation with a SNR of up to 5 in real time. These measurements represent the first demonstration that HTS rf SQUID multi-channel system may be applied practically to the measurements of fetal MCGs. We plan to extend the first-order gradiometer system to nine sensing channels.

Acknowledgment

The authors are grateful to H. Soltner, M. Mück, and A. I. Braginski for their critical remarks, suggestions and help with the preparation of the manuscript.

References

[1] A. H. Miklich, J. J. Kingston, F. C. Wellstood, J. Clarke, M. S. Colclough, K. Char, and G. Zaharchuk, *Nature*, vol. 352, pp. 482–484, 1991.
[2] Y. Zhang, Y. Tavrin, M. Mück, A. I. Braginski, C. Heiden, T. Elbert, and S. Hampson, *Clinical Phys. Physiol. Meas.*, vol. 14, pp. 113–116, 1993.
[3] Y. Tavrin, Y. Zhang, M. Mück, A. I. Braginski, and C. Heiden, *Appl. Phys. Lett.*, vol. 62, no. 15, pp. 1824–1826, 1993.
[4] F. Ludwig, E. Dantsker, D. Koelle, R. Kleiner, A. H. Miklich, and J. Clarke, *Appl. Supercond.*, vol. 3, pp. 383–385, 1995.
[5] Y. Zhang, N. Wolters, D. Lomparski, W. Zander, M. Banzet, H.-J. Krause, and P. van Leeuwen, *IEEE Trans. Appl. Supercond.*, vol. 13, no. 4, pp. 3862–3866, 2003.
[6] *Proc. 14th Int. Conf. Biomagnetism*, E. Halgren, S. Ahlfors, M. Hämäläinen, and D. Cohen, Eds., Boston, MA, 2004.
[7] H. Koch, *IEEE Trans. Appl. Supercond.*, vol. 11, no. 1, pp. 49–59, 2001.
[8] A. Tsukamoto, T. Fukazawa, K. Takagi, K. Yokosawa, D. Suzuki, and K. Tsukada, *Appl. Phys. Lett.*, vol. 79, pp. 4450–4453, 2001.
[9] *Proc. 14th Int. Conf. Biomagnetism*, E. Halgren, S. Ahlfors, M. Hämäläinen, and D. Cohen, Eds., Boston, MA, 2004, p. 662.
[10] Y. Zhang, J. Schubert, N. Wolters, M. Banzet, W. Zander, and H.-J. Krause, *Physica C*, vol. 372–376, pp. 282–285, 2002.
[11] M. J. Lewis, *Med. Eng. Phys.*, vol. 25, no. 10, pp. 801–810, 2003.
[12] P. van Leeuwen, S. Lange, A. Klein, D. Geue, Y. Zhang, H.-J. Krause, and D. Grönemeyer, *Physiol. Meas.*, vol. 25, pp. 539–552, 2004.